

An Immersed Boundary Method for Suspensions of Rigid Bodies

Aleksandar Donev, CIMS

&

Bakytzhan Kallemov and Florencio Balboa Usabiaga, CIMS
Boyce Griffith and Amneet Bhalla, UNC

Courant Institute, New York University

Numerical Analysis Seminar
Dec 5th 2014

Bent Active Nanorods

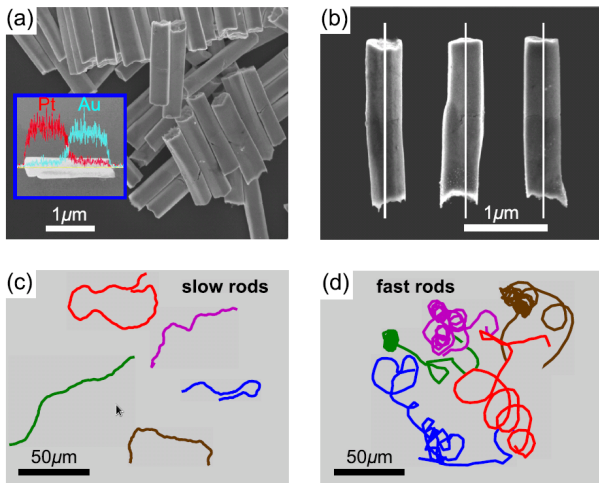
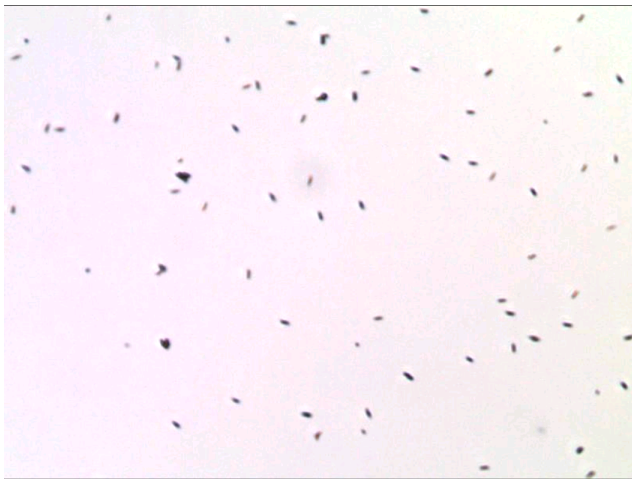


Figure: From the Courant Applied Math Lab of Zhang and Shelley [1]

Thermal Fluctuation Flips



QuickTime

Steady Stokes Flow ($\text{Re} \rightarrow 0$)

- Consider a **suspension of N_b rigid bodies** with positions $\mathcal{Q} = \{\mathbf{q}_1, \dots, \mathbf{q}_{N_b}\}$ and orientations $\Theta = \{\theta_1, \dots, \theta_{N_b}\}$. We describe orientations using quaternions but this will not be important in this talk.
- For viscous-dominated flows we can assume **steady Stokes flow** and define the **body mobility matrix** $\mathcal{N}(\mathcal{Q}, \Theta)$,

$$[\mathbf{U}, \mathbf{\Omega}]^T = \mathcal{N}[\mathcal{F}, \mathcal{T}]^T,$$

where the left-hand side collects the **linear** $\mathbf{U} = \{\mathbf{v}_1, \dots, \mathbf{v}_{N_b}\}$ and **angular** $\mathbf{\Omega} = \{\boldsymbol{\omega}_1, \dots, \boldsymbol{\omega}_{N_b}\}$ velocities, and the right hand side collects the **applied forces** $\mathcal{F}(\mathcal{Q}, \Theta) = \{\mathbf{F}_1, \dots, \mathbf{F}_{N_b}\}$ and **torques** $\mathcal{T}(\mathcal{Q}, \Theta) = \{\boldsymbol{\tau}_1, \dots, \boldsymbol{\tau}_{N_b}\}$.

Brownian Motion

- The **Brownian dynamics** of the rigid bodies is given by the **overdamped Langevin equation**

$$\begin{bmatrix} d\mathcal{Q}/dt \\ d\Theta/dt \end{bmatrix} = \begin{bmatrix} \mathcal{U} \\ \Omega \end{bmatrix} = \mathcal{N} \begin{bmatrix} \mathcal{F} \\ \mathcal{T} \end{bmatrix} + (2k_B T \mathcal{N})^{\frac{1}{2}} \diamond \mathcal{W}(t).$$

- **How to compute (the action of) \mathcal{N} and $\mathcal{N}^{\frac{1}{2}}$ and simulate the Brownian motion of the bodies?**
- This talk focuses on the deterministic aspects of computing \mathcal{N} and not on the stochastic aspects; but it all works together!
- We will also focus on passive rigid bodies but activity in the form of **active slip** or **active kinematics** can easily be incorporated.

Goals / Preview

Our methods are unique in that they:

- Work for the **steady Stokes regime** ($Re = 0$) as well as finite Reynolds numbers because there is **no time splitting**.
- **Strictly** enforce the **rigidity** constraint: **no penalty** parameters.
- Require **no Green's functions**, but rather, use a finite-volume staggered-grid **fluid solver** to include hydrodynamics.
- Ensure **fluctuation-dissipation balance** even in the presence of **nontrivial boundary conditions**.

Immersed Rigid Body

- In the **immersed boundary method** we extend the fluid velocity everywhere in the domain,

$$\rho \partial_t \mathbf{v} + \nabla \pi = \eta \nabla^2 \mathbf{v} + \int_{\Omega} \lambda(\mathbf{q}) \delta(\mathbf{r} - \mathbf{q}) d\mathbf{q} + \nabla \cdot \left(\sqrt{2\eta k_B T} \mathcal{W} \right)$$

$$\nabla \cdot \mathbf{v} = 0 \text{ everywhere}$$

$$m_e \dot{\mathbf{u}} = \mathbf{F} - \int_{\Omega} \lambda(\mathbf{q}) d\mathbf{q}$$

$$I_e \dot{\boldsymbol{\omega}} = \boldsymbol{\tau} - \int_{\Omega} [(\mathbf{q} - \boldsymbol{\rho}^0) \times \lambda(\mathbf{q})] d\mathbf{q}$$

$$\begin{aligned} \mathbf{v}(\mathbf{q}, t) &= \mathbf{v} + (\mathbf{q} - \boldsymbol{\rho}^0) \times \boldsymbol{\omega} \text{ for all } \mathbf{q} \in \Omega \\ &= \int \mathbf{v}(\mathbf{r}, t) \delta(\mathbf{r} - \mathbf{q}) d\mathbf{r}, \end{aligned}$$

where the **induced fluid-body force** [2] $\lambda(\mathbf{q})$ is a Lagrange multiplier enforcing the final **no-slip condition** (rigidity).

Immersed-Boundary Method

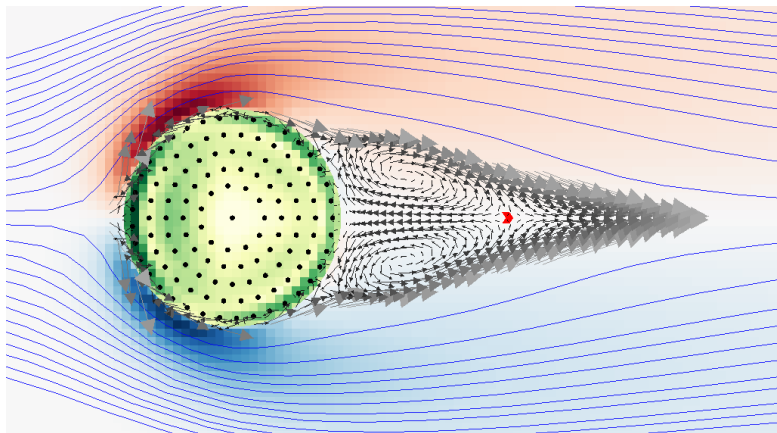


Figure: Flow past a rigid cylinder computed using our rigid-body immersed-boundary method at $Re = 20$. The cylinder is discretized using 121 markers/blobs.

Blob/Bead Models

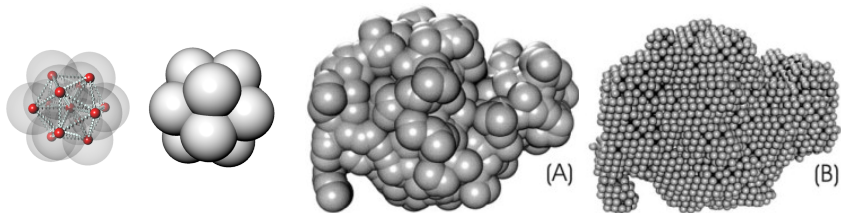


Figure: Blob or “raspberry” models of: a spherical colloid, and a lysozyme [3].

- The rigid body is discretized through a number of “**markers**” or “**blobs**” [4] with positions $\mathbf{Q} = \{\mathbf{q}_1, \dots, \mathbf{q}_N\}$.
- Composite velocity $\mathbf{U} = \{\mathbf{u}_1, \dots, \mathbf{u}_N\}$ and rigidity forces $\mathbf{\Lambda} = \{\lambda_1, \dots, \lambda_N\}$.

Blob Model

- Take an **Immersed Boundary Method** (IBM) approach and describe the fluid-blob interaction using a localized smooth **kernel** $\delta_a(r)$ with compact support of size a (*regularized delta function*).
- Define composite local *averaging* linear operator $\mathcal{J}(\mathbf{Q})$ operator, is the composite *spreading* linear operator, $\mathcal{S}(\mathbf{Q}) = \mathcal{J}^*(\mathbf{Q})$,

$$\mathbf{u}_i = (\mathcal{J}\mathbf{v})_i = \mathbf{J}_i\mathbf{v} = \int \delta_a(\mathbf{q}_i - \mathbf{r}) \mathbf{v}(\mathbf{r}, t) d\mathbf{r}$$

$$\boldsymbol{\lambda}(\mathbf{r}) = (\mathcal{S}\boldsymbol{\Lambda})(\mathbf{r}) = \sum_{i=1}^N \lambda_i \delta_a(\mathbf{q}_i - \mathbf{r}) = \sum_{i=1}^N \mathbf{S}_i \lambda_i.$$

In reality these are sums over grid points and δ_a is the **Peskin 6-pt kernel**.

Rigid-Body Immersed-Boundary Method

- **Rigidly-constrained NS** for a **neutrally-buoyant** body:

$$\rho \partial_t \mathbf{v} + \nabla \pi = \eta \nabla^2 \mathbf{v} + \sum_{i=1}^N \mathbf{S}_i \lambda_i + \sqrt{2\eta k_B T} \nabla \cdot \mathcal{W}$$

$$\nabla \cdot \mathbf{v} = 0 \quad (\text{Lagrange multiplier is } \pi)$$

$$\sum_i \lambda_i = \mathbf{F} \quad (\text{Lagrange multiplier is } \mathbf{v}) \quad (1)$$

$$\sum_i (\mathbf{q}_i - \boldsymbol{\varrho}^0) \times \lambda_i = \boldsymbol{\tau} \quad (\text{Lagrange multiplier is } \boldsymbol{\omega}),$$

$$\mathbf{J}_i \mathbf{v} = \mathbf{v} + \boldsymbol{\omega} \times (\mathbf{q}_i - \boldsymbol{\varrho}^0) + \text{slip} \quad (\text{Multiplier is } \lambda_i)$$

- 1 **Specified kinematics** (e.g., swimming object): Unknowns are \mathbf{v} , π and $\boldsymbol{\Lambda}$, while \mathbf{F} and $\boldsymbol{\tau}$ are outputs (easier).
- 2 **Free bodies** (e.g., colloidal suspension): Unknowns are \mathbf{v} , π and $\boldsymbol{\Lambda}$, \mathbf{v} and $\boldsymbol{\omega}$, while \mathbf{F} and $\boldsymbol{\tau}$ are inputs (harder).

Fluid Solver

- Discretize the fluid equation using the **staggered-grid (MAC)** second-order scheme on a uniform Cartesian grid with grid spacing h , using the discrete gradient \mathbf{G} , the discrete divergence $\mathbf{D} = -\mathbf{G}^*$, and the velocity Laplacian \mathbf{L} .
- After temporal discretization of the fluid equations, using backward Euler or Crank-Nicolson, we get

$$\frac{\rho}{\Delta t} \mathbf{I} - \eta \mathbf{L} \mathbf{v}$$

- Denote $\beta = \nu \Delta t / h^2 = \eta \Delta t / (\rho h^2)$ is the **viscous CFL number**, $\beta \rightarrow \infty$ for Steady stokes, $\beta = 0$ for inviscid, and define

$$\mathbf{A} = \eta h^{-2} (\beta^{-1} \mathbf{I} - h^2 \mathbf{L}).$$

The dimensionless matrix $\beta^{-1} \mathbf{I} - h^2 \mathbf{L}$ is essentially a discretization of an imaginary **Helmholtz** or **screened Poisson equation** and the action of \mathbf{A}^{-1} can be obtained using geometric multigrid.

Saddle-Point Problem

- Define the geometric matrix \mathcal{K} that converts body kinematics to marker kinematics,

$$\mathcal{K}\mathcal{Y} = \mathcal{K}[\mathbf{u}, \boldsymbol{\Omega}]^T = \mathbf{u} + \boldsymbol{\Omega} \times (\mathbf{Q} - \mathbf{Q}^0).$$

- After temporal discretization of the constrained NS equations, we get the **free-kinematics constrained Stokes saddle-point problem**,

$$\begin{bmatrix} \mathbf{A} & \mathbf{G} & -\mathcal{S} & \mathbf{0} \\ -\mathbf{D} & \mathbf{0} & \mathbf{0} & \mathbf{0} \\ -\mathcal{J} & \mathbf{0} & \mathbf{0} & \mathcal{K} \\ \mathbf{0} & \mathbf{0} & \mathcal{K}^* & \mathbf{0} \end{bmatrix} \begin{bmatrix} \mathbf{v} \\ \pi \\ \boldsymbol{\Lambda} \\ \mathcal{Y} \end{bmatrix} = \begin{bmatrix} \mathbf{g} \\ \mathbf{0} \\ \mathbf{0} \\ \mathcal{R} \end{bmatrix},$$

where $\mathcal{Y} = [\mathbf{u}, \boldsymbol{\Omega}]^T$ and $\mathcal{R} = [\mathcal{F}, \mathcal{T}]^T$, and recall that $\mathcal{S} = \mathcal{J}^*$.

- The **Stokes saddle-point problem**

$$\begin{bmatrix} \mathbf{A} & \mathbf{G} \\ -\mathbf{D} & \mathbf{0} \end{bmatrix} \begin{bmatrix} \mathbf{v} \\ \pi \end{bmatrix} = \begin{bmatrix} \mathbf{S}\boldsymbol{\Lambda} + \mathbf{g} \\ 0 \end{bmatrix},$$

using a **GMRES solver** with a **multigrid**-based projection-method preconditioner [5], to obtain

$$\begin{aligned} \mathbf{v} &= \mathcal{L}^{-1}(\mathbf{S}\boldsymbol{\Lambda} + \mathbf{g}) = \\ &= \left(\mathbf{A}^{-1} - \mathbf{A}^{-1}\mathbf{G}(\mathbf{D}\mathbf{A}^{-1}\mathbf{G})^{-1}\mathbf{D}\mathbf{A}^{-1} \right) (\mathbf{S}\boldsymbol{\Lambda} + \mathbf{g}), \end{aligned}$$

where the **Stokes solution operator** \mathcal{L}^{-1} is expressed in terms of the **Schur complement** $\mathbf{D}\mathbf{A}^{-1}\mathbf{G}$ of the saddle-point problem.

Specified Kinematics

- Let's first consider the simpler problem of **specified kinematics** (e.g., swimming fish) and the simpler **constrained Stokes saddle-point problem**:

$$\begin{bmatrix} \mathbf{A} & \mathbf{G} & -\mathcal{S} \\ -\mathbf{D} & \mathbf{0} & \mathbf{0} \\ -\mathcal{J} & \mathbf{0} & \mathbf{0} \end{bmatrix} \begin{bmatrix} \mathbf{v} \\ \pi \\ \boldsymbol{\Lambda} \end{bmatrix} = \begin{bmatrix} \mathbf{g} \\ 0 \\ -\mathcal{K}\mathcal{Y} \end{bmatrix}. \quad (2)$$

- The solution can be expressed in terms of the **Schur complement** \mathcal{M} ,

$$\boldsymbol{\Lambda} = \mathcal{M}^{-1} (\mathcal{K}\mathcal{Y} - \mathcal{J}\mathcal{L}^{-1}\mathbf{g}), \quad (3)$$

- The all-important $3N \times 3N$ block **mobility matrix** \mathcal{M} is

$$\mathcal{M} = \mathcal{J}\mathcal{L}^{-1}\mathcal{S},$$

and the main computational challenge will be to approximate the action of \mathcal{M}^{-1} for **preconditioning**.

Suspensions of Rigid Bodies

- The 3×3 block $\mathbf{M}_{ij} = \mathbf{J}_i \mathcal{L}^{-1} \mathbf{S}_j$ has a **simple physical interpretation**: It maps a force on marker j to a velocity of marker i .
- For steady Stokes flow

$$\mathcal{M}_{ij} \approx \eta^{-1} \int \delta_a(\mathbf{q}_i - \mathbf{r}) \mathbf{G}(\mathbf{r}, \mathbf{r}') \delta_a(\mathbf{q}_j - \mathbf{r}') \, d\mathbf{r} d\mathbf{r}' \quad (4)$$

where \mathbf{G} is the Green's function for the Stokes problem; **Oseen tensor** for an infinite domain.

- The **many-body mobility matrix** \mathcal{N} takes into account higher-order hydrodynamic interactions,

$$[\mathbf{U}, \mathbf{\Omega}]^T = \mathcal{N} [\mathcal{F}, \mathcal{T}]^T \quad \text{where} \quad \mathcal{N} = (\mathcal{K}^* \mathcal{M}^{-1} \mathcal{K})^{-1}.$$

Brownian Motion

- By adding the stochastic forcing $\nabla \cdot (\sqrt{2\eta k_B T} \mathcal{W})$ to the fluid equation we obtain the correct **fluctuating velocities** (Brownian motion),

$$\begin{bmatrix} \mathcal{U} \\ \mathcal{\Omega} \end{bmatrix} = \mathcal{N} \begin{bmatrix} \mathcal{F} \\ \mathcal{T} \end{bmatrix} + (2k_B T \mathcal{N})^{\frac{1}{2}} \diamond \mathcal{W},$$

where the “**square root**” of the mobility is **explicitly constructed** as

$$\mathcal{N}^{\frac{1}{2}} = \sqrt{2k_B T} \mathcal{N} \mathcal{K} \mathcal{M}^{-1} \mathcal{J} \mathcal{L}^{-1} \mathbf{D}_v \mathcal{W}.$$

- Observe that **discrete fluctuation-dissipation balance** is guaranteed,

$$\begin{aligned} \mathcal{N}^{\frac{1}{2}} \left(\mathcal{N}^{\frac{1}{2}} \right)^{\star} &= \mathcal{N} \mathcal{K} \mathcal{M}^{-1} (\mathcal{J} \mathcal{L}^{-1} \mathbf{L} \mathcal{L}^{-1} \mathcal{S}) \mathcal{M}^{-1} \mathcal{K}^{\star} \mathcal{N}, \\ &= \mathcal{N} (\mathcal{K} \mathcal{M}^{-1} \mathcal{K}) \mathcal{N} = \mathcal{N}. \end{aligned}$$

- This works for **confined systems**, **non-spherical** particles, and even **active particles**. Can also be extended to **semi-rigid structures** (e.g., bead-link polymer chains).

Iterative Solver

- The difficulty in the numerical method is solving the **large saddle-point system**:

$$\begin{bmatrix} \mathbf{A} & \mathbf{G} & -\mathcal{S} \\ -\mathbf{D} & \mathbf{0} & \mathbf{0} \\ -\mathcal{J} & \mathbf{0} & \mathbf{0} \end{bmatrix} \begin{bmatrix} \mathbf{v} \\ \pi \\ \Lambda \end{bmatrix} = \begin{bmatrix} \mathbf{g} \\ \mathbf{h} = \mathbf{0} \\ \mathbf{w} = -\mathcal{K}\mathcal{Y} \end{bmatrix}. \quad (5)$$

- We use an **iterative method** (FGMRES) preconditioned by using a **Schur complement approximation** in which we approximate \mathcal{M} analytically relying on **near translational-invariance** of the Peskin IB method [6].
- Fast direct solvers** (related to FMMs) are required to approximately compute the action of \mathcal{M}^{-1} .

Preconditioner

- 1 Solve the fluid sub-problem **approximately** (i.e., few multigrid sweeps) to obtain $\tilde{\mathbf{v}}$

$$\begin{bmatrix} \mathbf{A} & \mathbf{G} \\ -\mathbf{D} & \mathbf{0} \end{bmatrix} \begin{bmatrix} \tilde{\mathbf{v}} \\ \tilde{\pi} \end{bmatrix} = \begin{bmatrix} \mathbf{g} \\ \mathbf{h} \end{bmatrix}.$$

- 2 Solve **mobility sub-problem** $\mathbf{\Lambda} = -\tilde{\mathcal{M}}^{-1} (\mathcal{J}\tilde{\mathbf{v}} + \mathbf{w})$, where $\tilde{\mathcal{M}}^{-1} \approx \mathcal{M}^{-1}$ (key to efficiency!)
- 3 Solve the fluid subproblem again approximately:

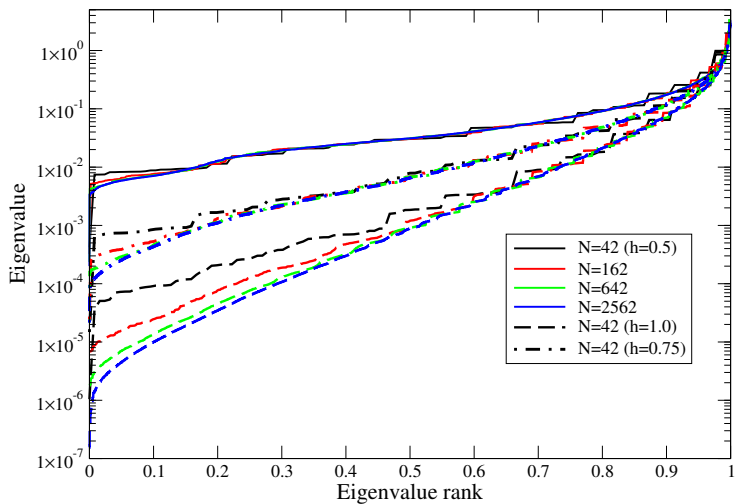
$$\begin{bmatrix} \mathbf{A} & \mathbf{G} \\ -\mathbf{D} & \mathbf{0} \end{bmatrix} \begin{bmatrix} \mathbf{v} \\ \pi \end{bmatrix} = \begin{bmatrix} \mathbf{g} + \mathcal{S}\mathbf{\Lambda} \\ \mathbf{h} \end{bmatrix}.$$

Well-Posedness

- The constrained Stokes system will be well-conditioned if the mobility matrix \mathcal{M} has a controlled conditioning number.
- We find that \mathcal{M} is **ill-conditioned if markers come closer than two grid cells apart**.
- This is not unexpected at all but it is different from usual IB wisdom for elastic bodies (markers half a grid cell apart).
- If markers are too far apart the flow “leaks” through the body.
- So for now we **keep markers two grid cells apart** and refine both fluid grid and marker grid in unison.
This should ensure a sort of LBB-like condition (?).
- We can do better if we combine with a finite-element method for the rigid body (see Outlook section)...

Spectrum of \mathcal{M}

Spherical shells (marker distance = 1)

solid $h=0.5$, dash-dotted $h=0.75$, dashed $h=1.0$ 

Approximating the mobility matrix

- The 3×3 **pairwise** block $\mathbf{M}_{ij} = \mathbf{J}_i \mathcal{L}^{-1} \mathbf{S}_j$ has a **simple physical interpretation**: force on marker $j \mapsto$ velocity of marker i .
- Idea #1: Ignore boundary conditions and consider an unbounded domain at rest at infinity.

Let the Krylov solver correct the errors due to ignoring the BCs.

- In principle, due to the presence of a fixed Eulerian grid, \mathbf{M}_{ij} depends on the positions of the marker relative to the grid. But Peskin's kernels are specifically construct to ensure **near translational invariance!**
- Idea #2: **Assume translational invariance** and approximate

$$\mathbf{M}_{ij} = \mathbf{J}_i \mathcal{L}^{-1} \mathbf{S}_j \approx \tilde{\mathbf{M}}_{ij} = f_\beta(r_{ij}) \mathbf{I} + g_\beta(r_{ij}) \hat{\mathbf{r}}_{ij} \otimes \hat{\mathbf{r}}_{ij},$$

where $\mathbf{r}_{ij} = \mathbf{r}_i - \mathbf{r}_j$, and $f_\beta(r)$ and $g_\beta(r)$ are two **kernel-dependent** functions of distance that depend on the viscous CFL number β .

Approximate pairwise mobility

- Use knowledge of Green's functions to model $f_\beta(r)$ and $g_\beta(r)$ with coefficients to be obtained by fitting numerical data.
- For example, for steady Stokes flow in 3D we know:
 - Self-mobility gives the effective hydrodynamic radius of the blob a (e.g., $a = 1.47 h$ for 6pt kernel),

$$f_\infty(0) = (6\pi\eta a)^{-1} \text{ and } g_\infty(0) = 0.$$

- Since Oseen tensor decays like $1/(8\pi\eta r)$, define the normalized functions

$$\begin{aligned}\tilde{f}(x) &= (8\pi\eta r) f(r) \\ \tilde{g}(x) &= (8\pi\eta r) g(r),\end{aligned}$$

where $x = r/h$ is the normalized distance between the blobs:

$$\tilde{f}(x \ll 1) \approx 4x/(3a/h) \text{ and } \tilde{g}(x \ll 1) = O(x^2)$$

$$\tilde{f}(x \gg 1) \approx \tilde{g}(x \gg 1) \approx 1.$$

Rotne-Prager-Yamakawa Mobility

The numerical data is well-fitted by the well-known Rotne-Prager-Yamakawa tensor commonly used in Brownian dynamics simulations:

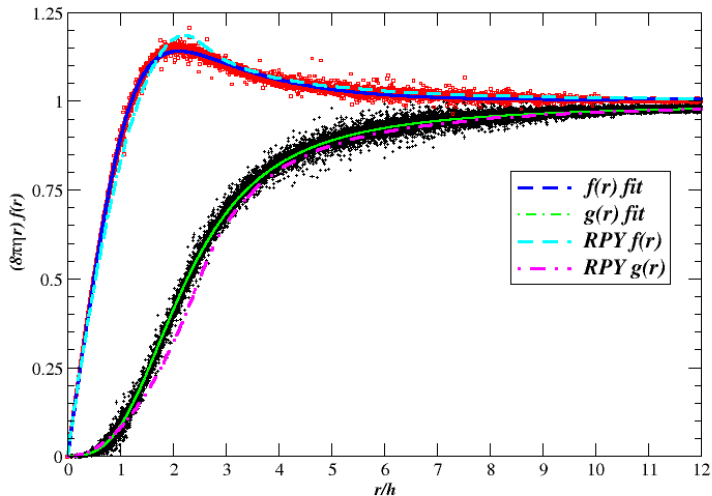
$$f(r) = \frac{1}{6\pi\eta a} \begin{cases} \frac{3a}{4r} + \frac{a^3}{2r^3}, & r > 2a \\ 1 - \frac{9r}{32a}, & r \leq 2a \end{cases} \quad (6)$$

and

$$g(r) = \frac{1}{6\pi\eta a} \begin{cases} \frac{3a}{4r} - \frac{3a^3}{2r^3}, & r > 2a \\ \frac{3r}{32a}, & r \leq 2a \end{cases} \quad (7)$$

An important property of the RPY mobility is that \mathcal{M} is guaranteed to be **symmetric positive semidefinite**.

Translational invariance (steady Stokes)



Empirical Mobility

- In practice we fit numerical data with semi-empirical rational functions that have the right asymptotic behavior:

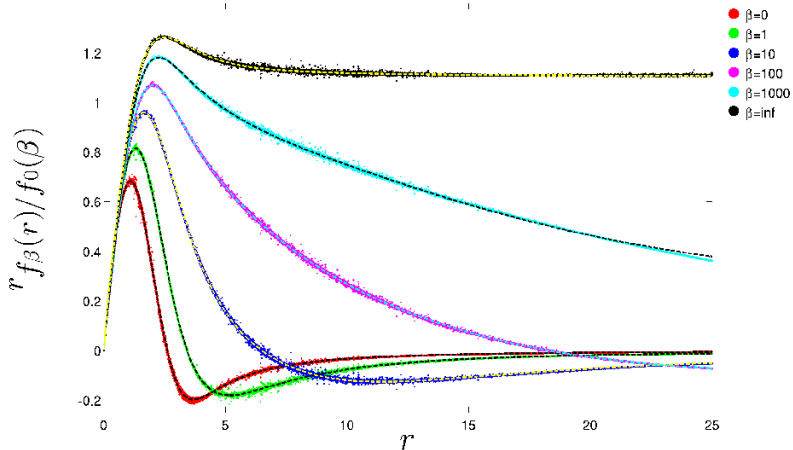
$$\tilde{f}(x) = b_1 x e^{-b_2 x} + \frac{b_3 x^2 + x^4}{1 + b_4 x^2 + x^4} \quad \text{if } x \geq 1$$

$$\tilde{g}(x) = \frac{x^3}{b_5 + b_6 x^2 + x^3}.$$

- Similar reasoning can be applied for the case of finite Reynolds number, for example, we can split the asymptotic behavior into an inviscid (dipole) and a viscid (monopole) term:

$$f_\beta(r \gg h) \sim -\frac{\beta}{\eta h} \left[\frac{1}{4\pi x^3} + \frac{1}{8\pi x \beta} \exp\left(-\frac{x}{C\sqrt{\beta}}\right) \right].$$

Translational invariance (unsteady Stokes)



Fast Solvers

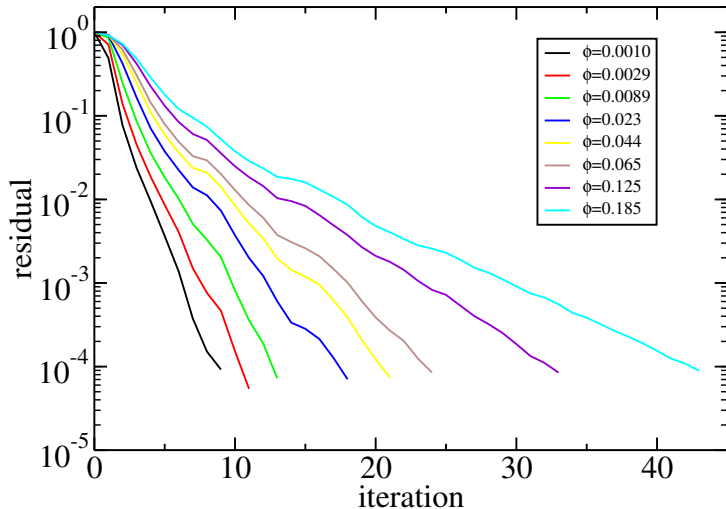
- After we approximate \mathcal{M} analytically, we still need to solve the linear system **approximately**

$$\mathcal{M}\Lambda = \mathbf{U}.$$

- For smallish number of markers we just use **dense direct** linear solvers (LAPACK). For large number of markers we need **application-specific approaches**.
- We have also had some success with the **HODLR low-rank approximation** fast solvers of Sivaram Ambikasaran (CIMS).
- An alternative is to use an iterative solver with **Fast Multipole Method** (we are using Leslie Greengard's codes) for the matrix vector-product, and a **body-block-diagonal preconditioner** (one dense diagonal block per rigid body).
- Presently working with the group of Eric Darve (Stanford) to develop better low-rank (HODLR) approximate factorizations to be used as a preconditioner for the FMM-based iterative solver...

FMM + Block-Diagonal Preconditioner

lattice (8,8,8) of shells with N=42 blobs

several volume fraction ϕ , always with Cholesky-preconditioner

Convergence

- We have implemented this method using the IBAMR software framework developed by Boyce Griffith: **RigidIBAMR**.
- We have tested the solver on some examples of zero and finite Reynolds number flows in 2D and 3D for which analytical answers are known, e.g., a moving sphere inside a stationary fixed shell (shell-in-shell or sphere-in-shell test) for steady Stokes.
- We **observe strong convergence** of the force density on the surface of the inner sphere as we refine the grid but the convergence is **only first-order** (as expected) and quite **slow**, and very sensitive to the marker spacing due to ill-conditioning.
- It appears **weak convergence** (of stress moments) is much more robust and rapid: most important for suspensions and obtaining qualitatively correct physics for **minimally-resolved** or **coarsely-resolved models**.

Shell-in-Shell Test

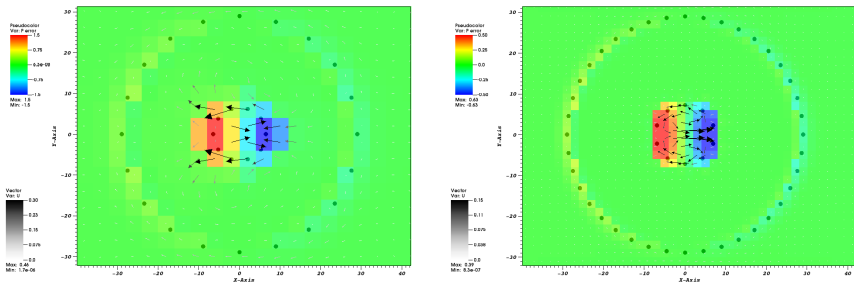


Figure: Error in the velocity and pressure for different resolutions. (Left) Outer: 162, Inner: 12 blobs. (Right) Outer: 642, Inner: 42 blobs.

Steady Stokes Test

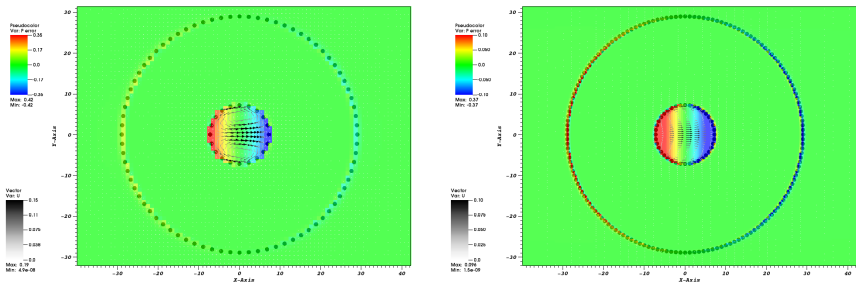


Figure: Error in the velocity and pressure for different resolutions. (Left) Outer: 2562, Inner: 162 blobs. (Right) Outer: 10242, Inner: 642 blobs.

Alternative Discretizations

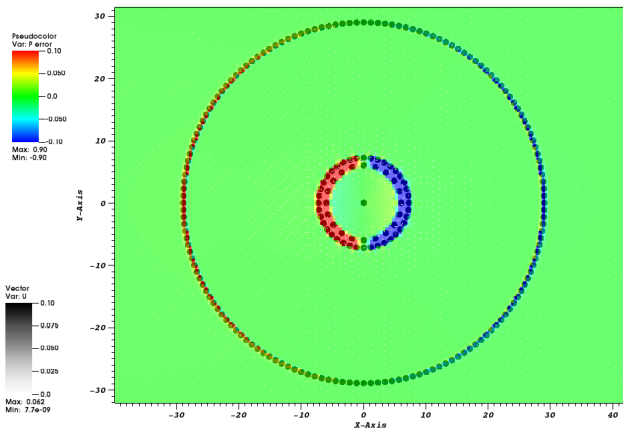


Figure: Error in the velocity and pressure for shell-in-shell steady Stokes test with double-shell.

Strong Accuracy

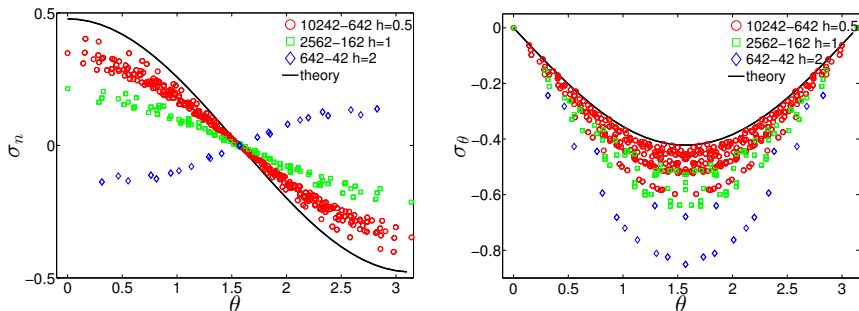


Figure: Convergence of surface stresses to their theoretical values for the three finest resolutions. (*Left*) Normal component of stress $\sigma \cdot \mathbf{n}$, $\sigma_{ij} \hat{r}_j \hat{r}_j$. (*Right*) Tangential component of stress in direction of flow $\sigma_{ij} \hat{r}_j \hat{\theta}_j$.

Sphere in Shear Flow

- The **low-order moments** of the fluid-particle stress converge relatively rapidly.
- The total **drag** (zeroth moment) and **torque** (antisymmetric part of the second moment),

$$\mathbf{F} = \sum_i \boldsymbol{\Lambda}_i \text{ and } \boldsymbol{\tau} = \sum_i \boldsymbol{\lambda}_i \times \mathbf{r}_i.$$

These are nonzero and consistent even for a **single blob**.

- But to get a nonzero **stresslet** (symmetric part of the second moment) we need a raspberry-type model,

$$\mathbf{S} = \text{SymmTraceless} \left\{ \sum_i \boldsymbol{\lambda}_i \otimes \mathbf{r}_i \right\}.$$

Weak Accuracy

- Compare to theoretical formulae to derive an effective hydrodynamic radius:

$$\mathbf{T} = 8\pi\mu R^3\boldsymbol{\omega} \text{ where } \boldsymbol{\omega} = (\nabla \times \mathbf{v})/2 \quad (8)$$

$$\mathbf{S} = \frac{10\pi}{3}\eta R^3\dot{\boldsymbol{\gamma}} \text{ where } \dot{\boldsymbol{\gamma}} = \nabla\mathbf{v} + \nabla^T\mathbf{v}.$$

# blobs	Drag R_h	Torque R_τ	Stresslet R_s	Geom R_g
12	1.4847	1.3774	1.4492	1
42	1.2152	1.1671	1.2474	1
162	1.0864	1.0730	1.0959	1
642	1.0377	1.0343	1.0405	1
2562	1.0172	1.0163	1.0184	1

Table: Hydrodynamic radii for several resolutions of shell sphere models.

Lubrication forces

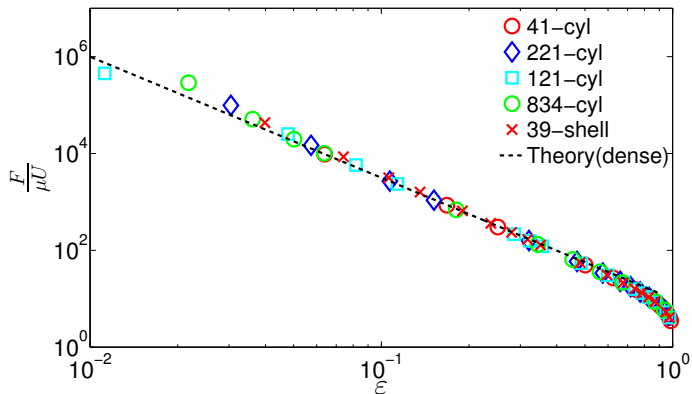


Figure: The drag coefficient for a periodic array of cylinders in steady Stokes flow for close-packed arrays with inter-particle gap ε , showing the correct asymptotic $\varepsilon^{-5/2}$ lubrication force divergence.

Finite Reynolds number

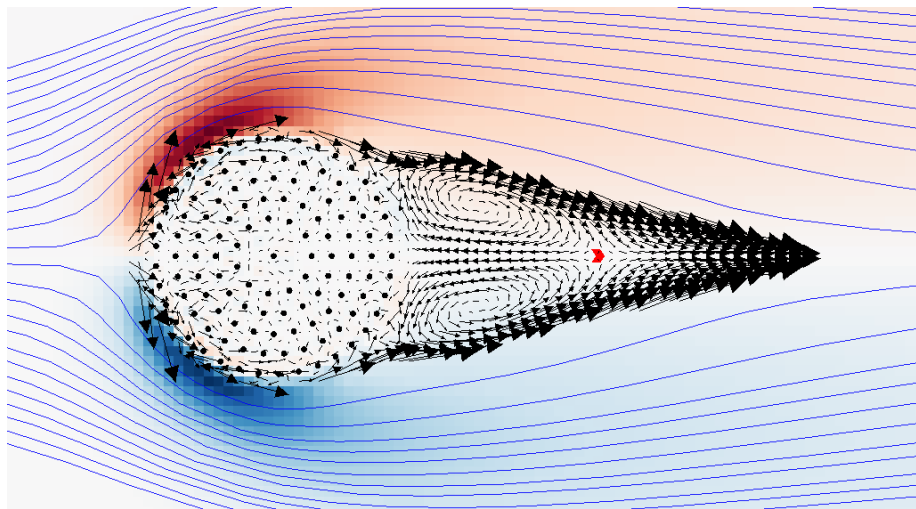


Figure: Flow past a rigid 121-marker cylinder at $Re = 20$ (drag matches literature up to $Re = 100$).

Comparison to other methods

- At the level of the formulation, for steady Stokes flow this is very similar to existing methods, e.g., **Regularized Stokeslets**. Main difference is that the mobility matrix in our formulation is SPD.
- It also looks like a **regularized first-kind boundary-element** formulation (so not very good!). Leslie Greengard and Manas Rachh are developing better second-kind methods but thermal fluctuations require a bit more work.
- The main difference with above is that **we do not use Green's functions** but rely on a fluid solver; this works with various **boundary conditions, finite Reynolds numbers, variable viscosity flows**.
- Unlike **Stokesian dynamics** and related multipole-based methods such as **Force Coupling Method** this approach has **controlled accuracy** (no *ad hoc* lubrication), but also more expensive.
- The treatment of thermal fluctuations is similar to that in the popular **Lattice Boltzmann Method** but the fluid solver here is very different (allowing zero Reynolds and Mach numbers, for example).

FEM (Filtering)

- We are presently working on using a **Finite Element method** to represent the rigid body and the induced force density $\lambda(\mathbf{q})$ using standard FEM basis functions.
- In this approach by Boyce Griffith the IB markers are placed at the Gauss nodes of the FEM mesh.
- Algebraically this amounts to transforming the Schur complement from \mathcal{M} to the **filtered mobility**

$$\mathcal{M}_{FE} = \Psi \mathcal{M} \Psi^T,$$

where Ψ is a sparse FEM assembly matrix that connects nodes of the grid to Gauss points.

- This filtering decreases the number of DOFs and **improves the conditioning dramatically**, and may lead to much improved strong convergence (but **still first order**).
- Effective preconditioning needs to be developed...

Future Directions

- Develop fast solvers for RPY-like kernels (with Eric Darve)
- Incorporate thermal fluctuations and develop stochastic integration algorithms (in progress).
- Develop formulations more akin to (regularized) second-kind integral equations to get improved accuracy and conditioning.
- Do active-body suspension applications (volunteers?).

References



Daisuke Takagi, Adam B Braunschweig, Jun Zhang, and Michael J Shelley.
Dispersion of self-propelled rods undergoing fluctuation-driven flips.
Phys. Rev. Lett., 110(3):038301, 2013.



D. Bedeaux and P. Mazur.
Brownian motion and fluctuating hydrodynamics.
Physica, 76(2):247–258, 1974.



José García de la Torre, María L Huertas, and Beatriz Carrasco.
Calculation of hydrodynamic properties of globular proteins from their atomic-level structure.
Biophysical Journal, 78(2):719–730, 2000.



F. Balboa Usabiaga, R. Delgado-Buscalioni, B. E. Griffith, and A. Donev.
Inertial Coupling Method for particles in an incompressible fluctuating fluid.
Comput. Methods Appl. Mech. Engrg., 269:139–172, 2014.
Code available at <https://code.google.com/p/fluum>.



M. Cai, A. J. Nonaka, J. B. Bell, B. E. Griffith, and A. Donev.
Efficient Variable-Coefficient Finite-Volume Stokes Solvers.
16(5):1263–1297, 2014.
Comm. in Comp. Phys. (CiCP).



B. Kallemov, A. Pal Singh Bhalla, B. E. Griffith, and A. Donev.
An immersed boundary method for suspensions of rigid bodies.
In preparation, to be submitted to *Comput. Methods Appl. Mech. Engrg.*, 2015.